https://doi.org/10.1007/s11467-023-1376-1

RESEARCH ARTICLE

Tunable near-infrared light emission from layered TiS_3 nanoribbons

Junrong Zhang[1,2], Cheng Chen[1,2], Yanming Wang[1,2], Yang Lu[1,2], Honghong Li[3], Xingang Hou[2], Yaning Liang[2,4], Long Fang[2,5], Du Xiang[3,†], Kai Zhang[1,2,‡], Junyong Wang[1,2,#]

[1]School of Nano-Tech and Nano-Bionics, University of Science and Technology of China, Hefei 230026, China

[2]CAS Key Laboratory of Nanophotonic Materials and Devices & Key Laboratory of Nanodevices and Applications, i-Lab, Suzhou Institute of Nano-Tech and Nano-Bionics (SINANO), Chinese Academy of Sciences, Suzhou 215123, China

[3]Frontier Institute of Chip and System, Fudan University, Shanghai 200438, China

[4]School of Materials Science and Engineering, Shanghai University, Shanghai 200444, China

[5]Inner Mongolia Univ Technol, Coll Energy & Power Engn, Hohhot 010051, China

Corresponding authors. E-mail: †xiang_du@fudan.edu.cn, ‡kzhang2015@sinano.ac.cn, #jywang2022@sinano.ac.cn

Received October 20, 2023; accepted November 30, 2023

Supporting Information

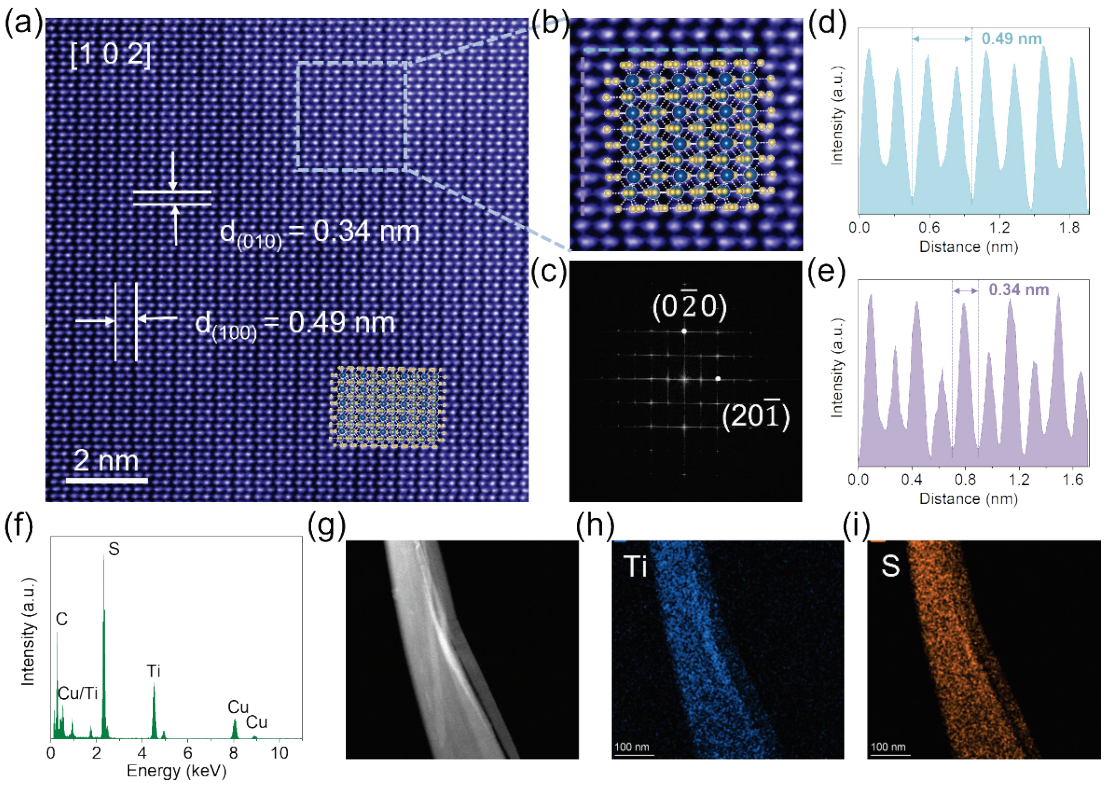

Fig. S1 TiS_3 nanoribbons with high crystallinity. **(a, b)** High-resolution HAADF-STEM images of the TiS_3 nanoribbon. **(c)** Corresponding SAED pattern of the TiS_3 nanoribbon. **(d, e)** Intensity profile of the blue and pink dashed lines in (e), respectively. **(f)** Energy-dispersive spectroscopy (EDS) spectrum of TiS_3 nanoribbon. **(g)** HAADF image of a TiS_3 nanoribbon. **(h, i)** EDS elemental mappings of Ti and S, respectively.

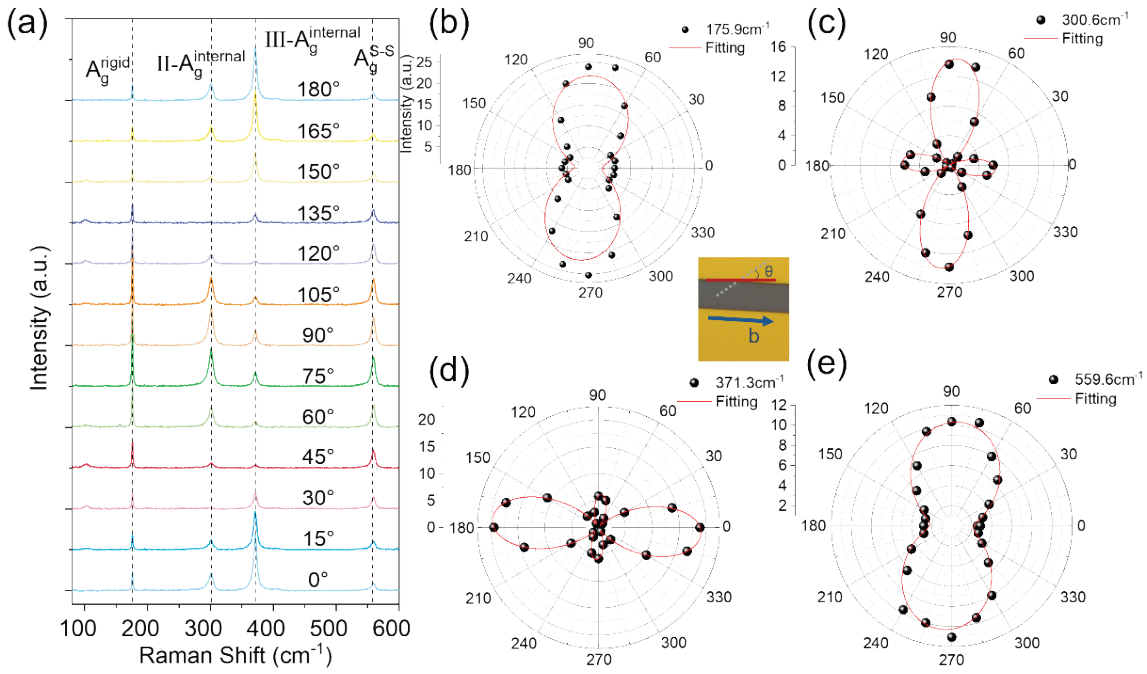

Fig. S2 Angle-dependent Raman spectra of TiS_3 nanoribbons. **(a)** Angle-resolved Raman spectra of TiS_3 flake evolving with angle. **(b–e)** Polar plot of 175.9 cm^{-1}, 300.6 cm^{-1}, 371.3 cm^{-1} and 559.6 cm^{-1} mode intensity. 175.9 cm^{-1}, 559.6 cm^{-1} mode are two-lobe shape, and 300.6 cm^{-1}, 371.3 cm^{-1} mode is four-lobe shape. The black spots are experimental results, and the red solid lines are fitted results.

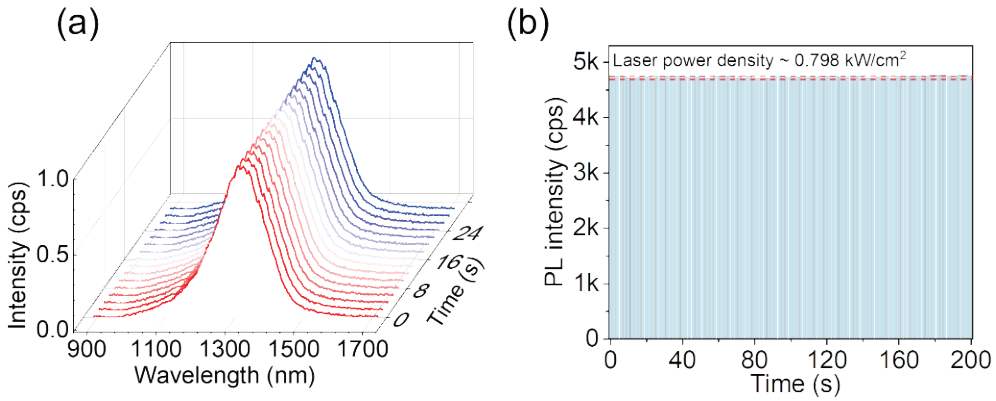

Fig. S3 (a) Near-infrared PL spectra of TiS_3 nanoribbon as a function of laser exposure time from the intrinsic emission. **(b)** PL intensity as a function of laser exposure time.

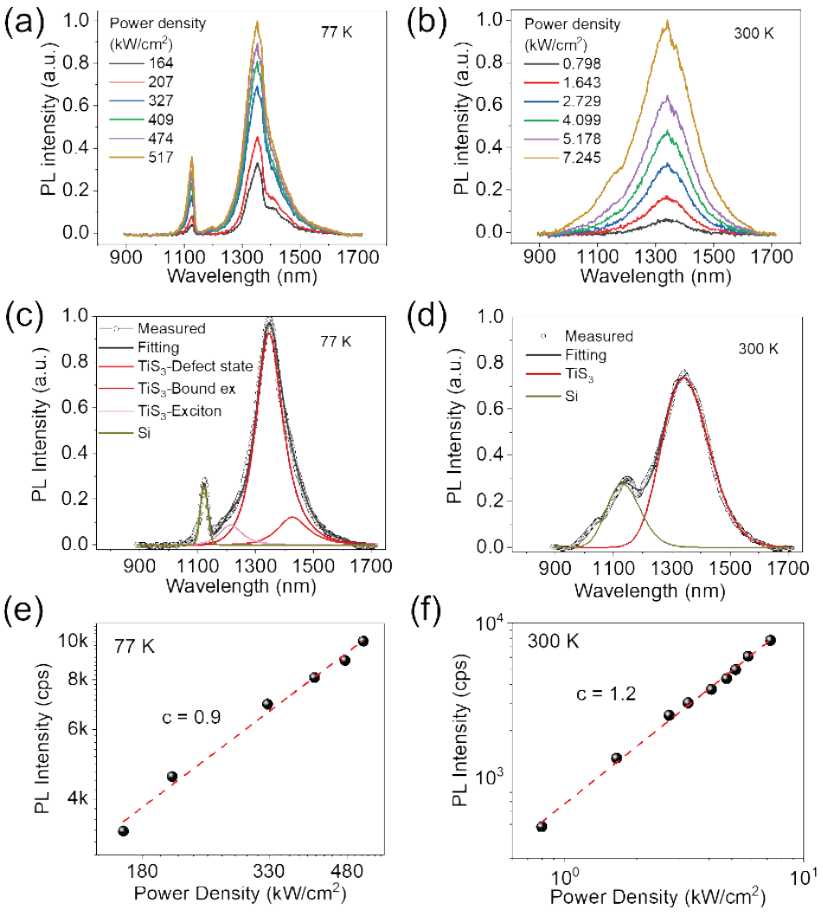

Fig. S4 (a, b) Photoluminescence spectra of TiS_3 nanoribbon as a function of laser power density under 77 K and 300 K. **(c, d)** Detailed spectra of the emission pattern, showing the TiS3 nanoribbon (red lines) peak and Si (green line) peak under 77 K and 300 K. **(e, f)** Excitation power density dependent spectral integral PL intensity measured at 77 K and 300 K for the entire spectra, the red dotted lines are power-law fittings.

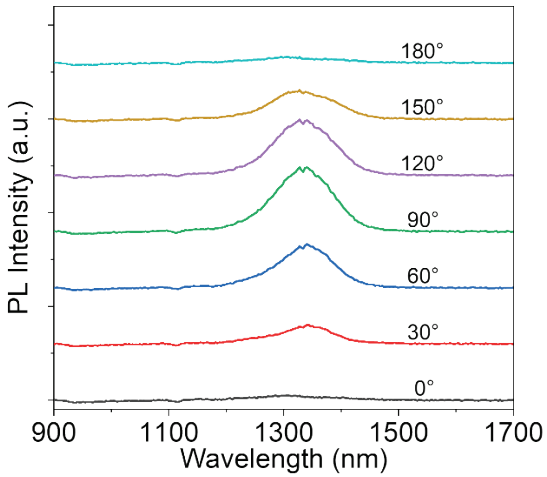

Fig. S5 Angle-resolved PL spectra of TiS_3 flake evolving with angle.

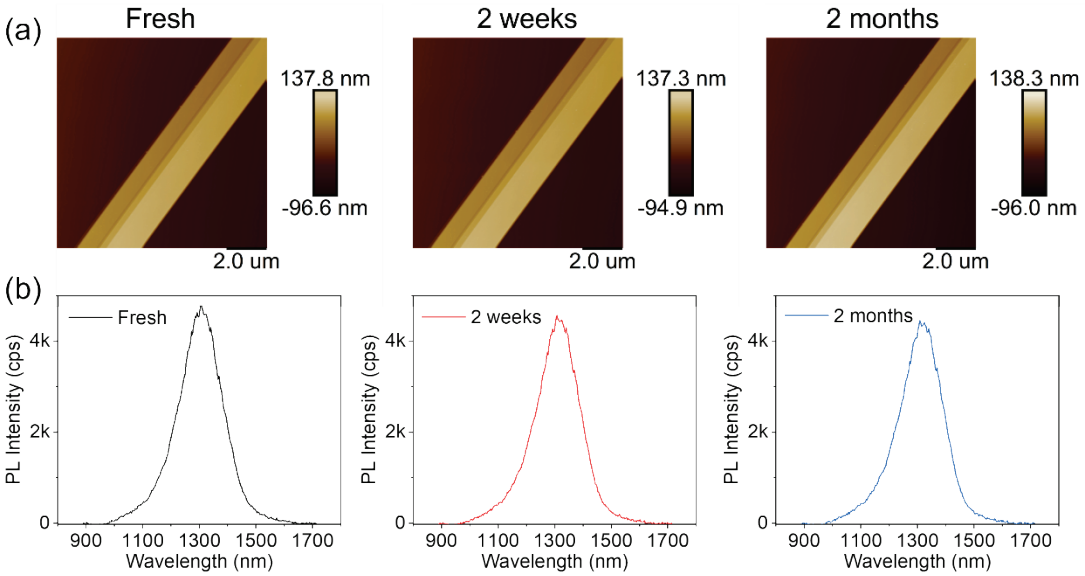

Fig. S6 (a) Time-dependent AFM images of TiS_3 nanosheets placed in the environment. **(b)** The corresponding photoluminescence spectra at different times.

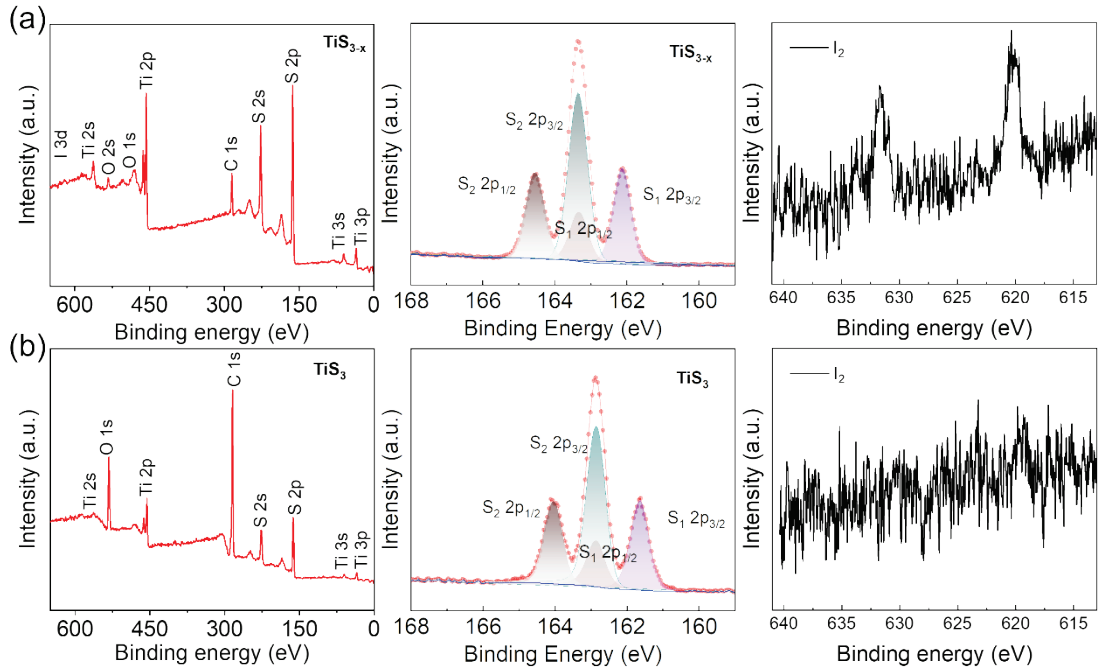

Fig. S7 XPS spectra of **(a)** wide-scan, **(b)** S 2p, and **(c)** I 3d for TiS_{3-x} and TiS_3.

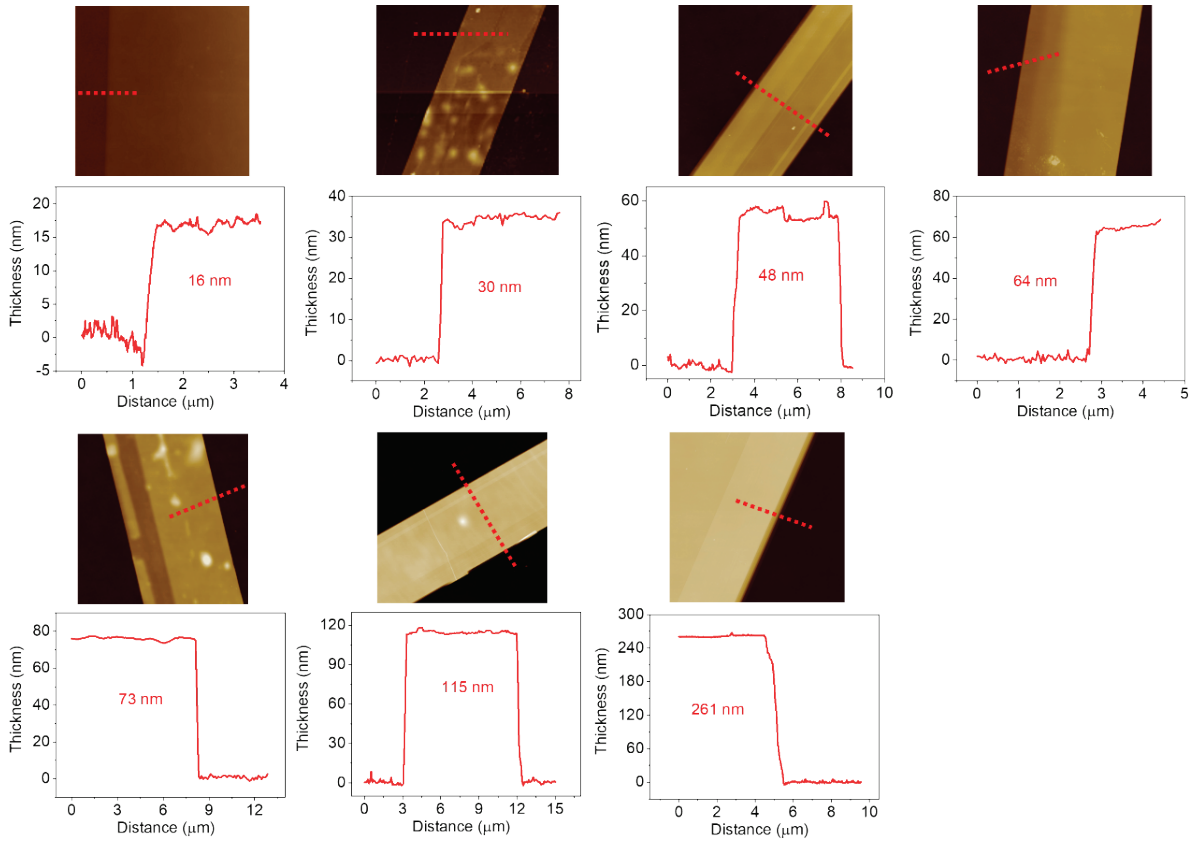

Fig. S8 AFM images (top) and their thickness results (bottom).

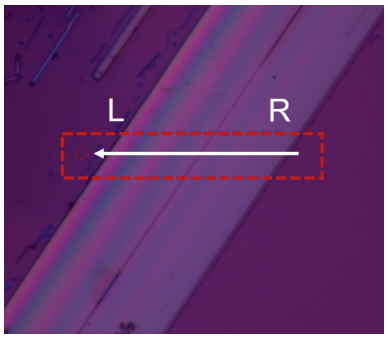

Fig. S9 The optical diagram of TiS_3 nanosheet with gradient thickness.

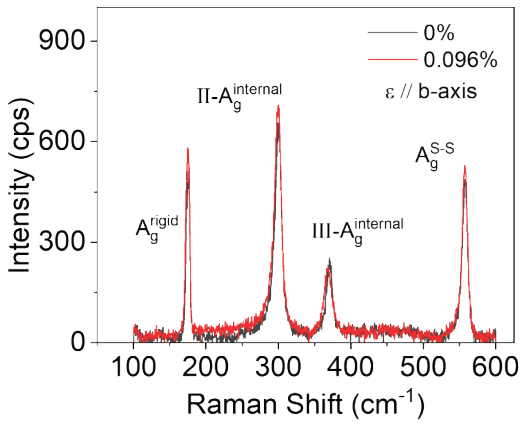

Fig. S10 Raman spectra of TiS_3 that encapsulated by PMMA under the uniaxial strain along the *b*-axis direction.

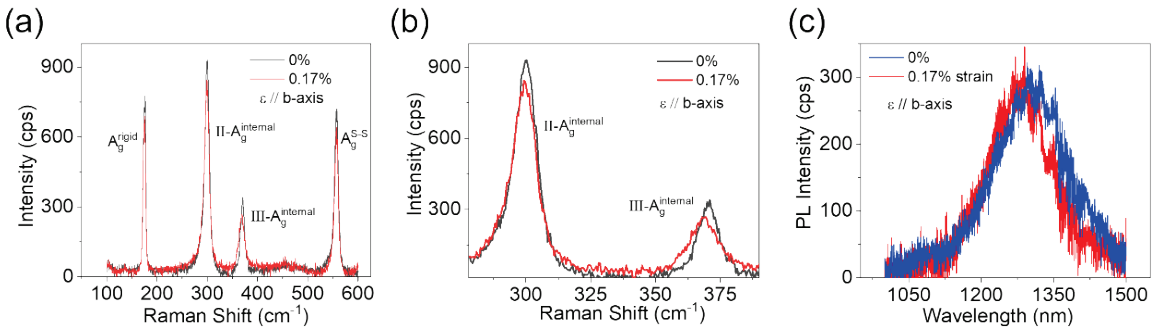

Fig. S11 Another device applies strain along the *b*-axis. **(a)** Evolution of the Raman spectra of the encapsulated TiS_3 nanoribbon on PET substrate under the uniaxial strain along the *b*-axis. **(b)** Enlarged Raman spectra in (a). **(c)** Evolution of the PL spectra of the encapsulated TiS_3 nanoribbon on PET substrate under the uniaxial strain along the *b*-axis.

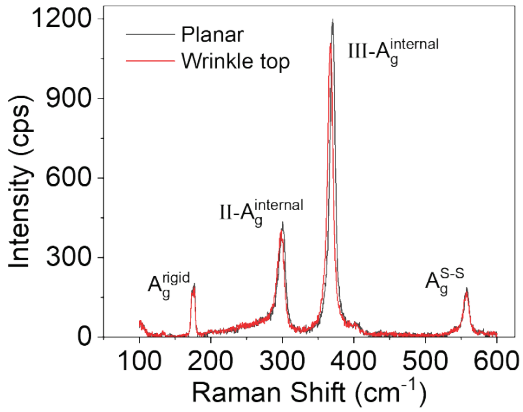

Fig. S12 Raman spectra were measured on the planar region and the top of the wrinkle region on a TiS_3 nanoribbon.

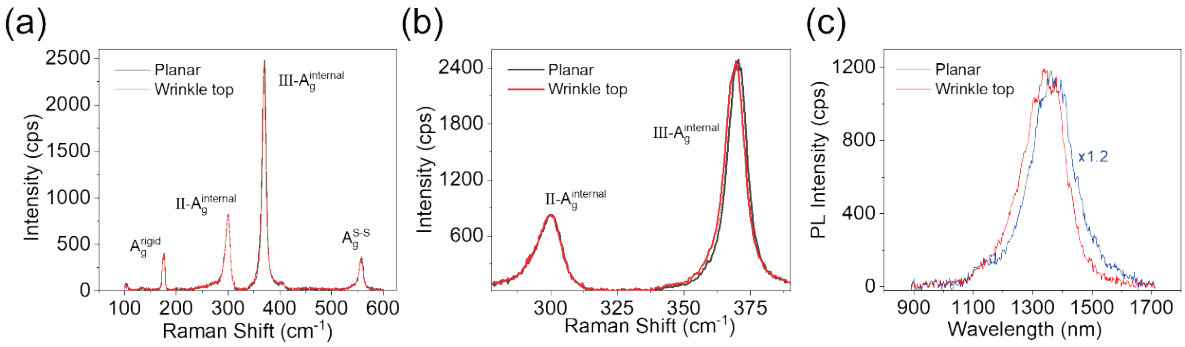

Fig. S13 Another TiS_3 nanoribbon with a wrinkle region along the *b*-axis. **(a)** The evolution of the Raman spectra was measured on the planar region and the top of the wrinkle region. **(b)** Enlarged Raman spectra in (a). **(c)** The evolution of the PL spectra was measured on the planar region and the top of the wrinkle region.